Alcántara García, A., García Casas, A. y Jiménez Morales, A. (2018). Electrochemical study of the synergic effect of phosphorus and cerium additions on a sol-gel coating for Titanium manufactured by powder metallurgy. *Progress in Organic Coatings,* 124, pp. 267-274.

DOI: 10.1016/j.porgcoat.2018.01.026

Electrochemical study of the synergic effect of phosphorus and cerium additions on a sol-gel coating for Titanium manufactured by powder metallurgy

Andrea Alcantara-Garcia[a,*], A. Garcia-Casas[a], A. Jimenez-Morales[a,b]

[a] Departamento de Ciencia e Ingeniería de Materiales e Ingeniería Química Universidad Carlos III de Madrid, Av. Universidad, 30, 28911, Leganés, Madrid, Spain
[b] Instituto Tecnológico de Química y Materiales Alvaro Alonso Barba, de la Universidad Carlos III de Madrid, Spain

ARTICLE INFO

Keywords: Corrosion Sol-gel Coatings EIS Inhibitors Titanium

ABSTRACT

The goal of this work was to combine the physical barrier properties provided by the sol-gel network with an active-chemistry protection against corrosion provided by corrosion inhibitors and cross-linking agents. Sol-gel coatings, organic–inorganic hybrid materials were prepared by hydrolysis and condensation of (3-glycidylox-ypropyl)trimethoxysilane (GPTMS) and tetraethylorthosilane (TEOS) in an ethanol/water solution. This coatings were satisfactorily modified by adding an inhibitor of the corrosion, namely hexahydrate cerium nitrate, and a cross-linking agent, namely tris(trimethylsilyl)phosphite (TMSP). The synergetic effect of these two compounds was evaluated by means of electrochemical characterization. The evolution rate of the hydrolysis-poly-condensation reaction was monitored by Fourier-transform infrared spectroscopy and viscosity. Once the hy-drolysis-polycondensation rate was reached, sols were deposited on titanium fabricated by powder metallurgy. The morphological characteristics and elemental distribution of the coatings were studied using scanning electrochemical microscopy (SEM). The solid-state of Si-NMR spectroscopy and thermogravimetric analysis (TGA) was employed in order to identify the cross-linking state of the coating by ensuring the creation of enough siloxane bonds. Impedance measurements were carried out to study the effect of cerium and TMSP on the corrosion resistance. It was observed that the coating with additions of cerium presented stable and good barrier features against 5 mM NaCl solution. The synergy between the cerium inhibitor and the TMSP cross-linking agent was found not to exert a positive effect because the electrochemical behaviour was dominated by the phosphorus compound over the cerium.

1. Introduction

Due to its high strength, low density, excellent corrosion resistance and biocompatibility with the human body, titanium is an attractive structural material considerably used in several sectors such as aeronautical, aerospace, automobile industry and medical applications [1–3]. The main issues concerning the use of titanium are the costs associated with the mineral extraction and the complex procedure to avoid its contamination. Several works are currently developing alternative procedures for titanium. Amherd Hidalgo, A. et al. [4] provided an extended review of how to enhance the sintering step of titanium by alloying titanium with copper, nickel or iron. Neves, R. G. et al. [5] designed powders of titanium by combining a conventional powder metallurgy procedure with colloidal techniques. Due to the strong affinity that Ti has to oxygen, nitrogen and carbon, sintering is performed under high vacuum to avoid the precipitation of intermetallics [4,6,7].

In order to protect, maintain and prolong the properties of metals, hybrid organic-inorganic sol-gel coatings have been source of attention from the past decades [8–10]. This materials represent an environmentally friendly alternative for chromate coatings, which have been forbidden in Europe since 2007 due to their highly carcinogenic effect [11]. Hybrid organic-inorganic coatings can act as a barrier layer to isolate metallic substrates from its environment [12], however, sometimes they fail to protect substrates once the coating is damaged. The challenge in this field is to combine the physical barrier properties provided by the sol-gel network with an active-chemistry protection against corrosion provided by corrosion inhibitors, cross-linking agents or both of this substances [13].

Sol-gel technology is a chemical synthesis process that creates an organic-inorganic coating that can effectively accommodate different protective substances against corrosion for the performance of materials [8,14]. However, introducing this corrosion inhibitors/cross-

* Corresponding author at: Materials Science and Engineering Department. Universidad Carlos III of Madrid, Avda. Universidad 30, 28911 Leganés, Madrid, Spain.
E-mail addresses: andrea.alcantara@uc3m.es (A. Alcantara-Garcia), amagarci@ing.uc3m.es (A. Garcia-Casas), toni@ing.uc3m.es (A. Jimenez-Morales).

Table 1
Summary of the sol-gel doped.

Nomenclature	Component	Silanes:component/ molar ratio	wt.% of component
Control	–	–	–
Ce	$Ce(NO_3)_3{\cdot}6H_20$	–	0.2
TMSP	tris(trimethylsilyl) phosphite	200/1	–
Ce + TMSP	$Ce(NO_3)_3{\cdot}6H_20$ + tris (trimethylsilyl) phosphite	200/1	0.2

Table 2
Assignment of FTIR peaks of Fig. 1.

Wavenumber (cm^{-1})	Assignment
3100–3700	υ(O—H)
3000–2900	υ(C—H)
1636	δ(O—H)
1500–1300	δ(C—H)
1250–1000	υ(Si—OH)
	υ(Si—C)
1187	υ(Si—O—Si)
1100–1070	υ (Si—O—C)

linking agents could compromise the stability of the sol-gel matrix, and also create cracks on the coating surface during the drying step. In order to avoid or minimized these issue, the optimization of the sol-gel procedure must be done by modifying different parameters of the procedure (i.e., the weight percentage of the substances added, the synthesis time, the viscosity of the sol prior to deposition, the curing time and temperature).

In this work two alcoxysilanes (GPTMS and TEOS) were used to prepare a sol-gel coating. Two strategies were employed to provide the coating with (1) physical barrier feature by adding a cross-liking agent and (2) active-chemistry protection with a controlled deliver of an inhibitor. Cross-linking agents are compounds that contribute to the formation of the sol-gel network. They can react with the alcoxysilanes and form covalent bonds. Cross-linking agents improve the adhesion between incompatible inorganic surface and/or organic polymers through intra or intermolecular reaction [15]. Several articles [16–18] confirm the improvement on the corrosion protection of magnesium alloys by applying a sol-gel coating doped with tris(trimethylsilyl) phosphite. This improvement on the corrosion protection is associated

Table 3
Mean viscosity values calculated for each synthesis.

Reaction time (h)	Viscosity (mPa s)			
	Control	Ce	TMSP	Ce + TMSP
1	4.6 ± 0.2	4.3 ± 0.4	4.1 ± 0.2	5.1 ± 0.3
8	4.4 ± 0.4	4.3 ± 0.7	4.9 ± 0.3	4.8 ± 0.3
24	5.6 ± 0.5	5.9 ± 0.3	9.3 ± 0.4	8.0 ± 0.4
48	9.4 ± 0.4	10.9 ± 0.5	25.2 ± 1.2	18.5 ± 0.9
72	40.0 ± 2.0	45.8 ± 2.0	130.8 ± 8.0	57.6 ± 3.0

with the formation of hydrolytically stable Mg—O—P chemical bonds. Concerning inhibitors, a wide range of substances has been employed to inhibit the corrosion of metals such as aluminum [19] and steel [13,30]. An excellent alternative for replacing Cr(VI) consist on the addition of rare earth elements. Lanthanide ions such as Ce^{3+}, Y^{3+}, La^{3+}, Pr^{3+}, Nd^{3+} seem to fulfil the basic requirements as alternative corrosion inhibitors by providing remarkable adhesion promotion, good barrier properties and self-healing properties [16,11,21].

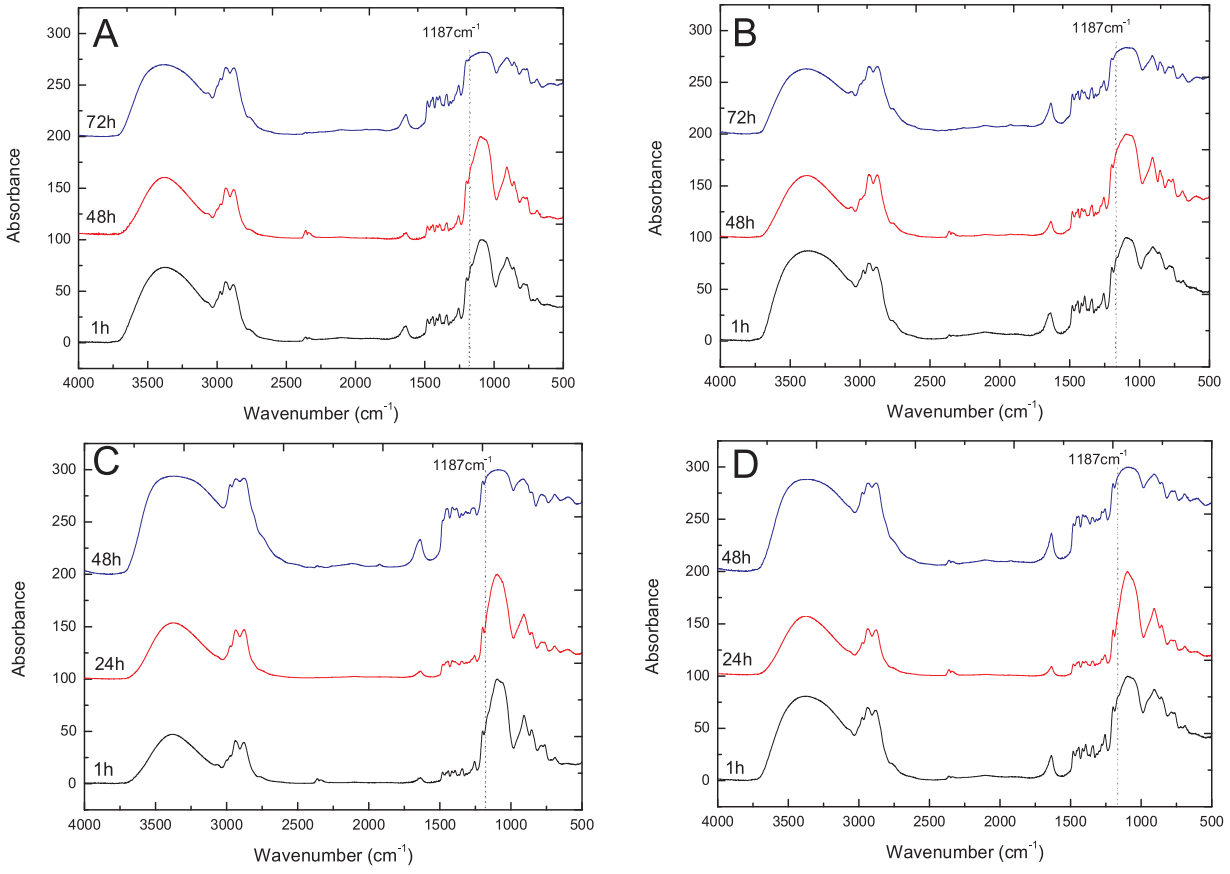

Fig. 1. FTIR spectra of synthesis: (A) Control, (B) Ce, (C) TMSP and (D) Ce + TMSP at different reactions times (from 1 h to 72 h).

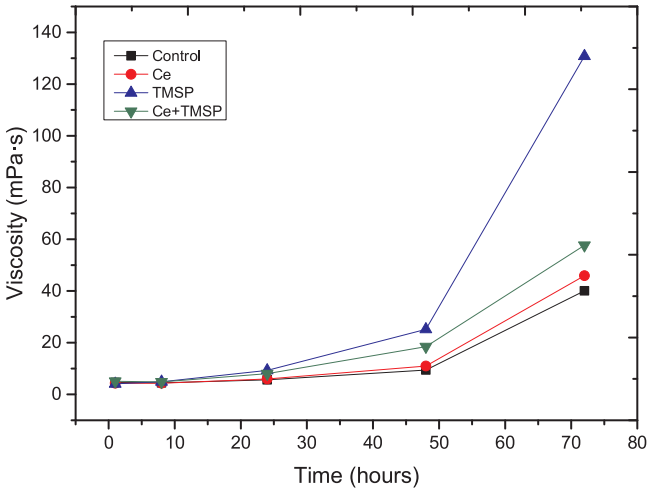

Fig. 2. Relation between viscosity and time of sols from synthesis Control, Ce, TMSP and Ce + TMSP.

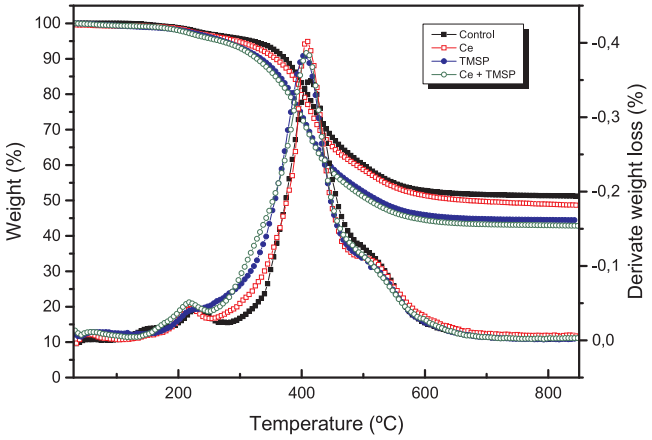

Fig. 3. TGA and TGA derivate curves of dry gels of Control, Ce, TMSP and Ce-TMSP.

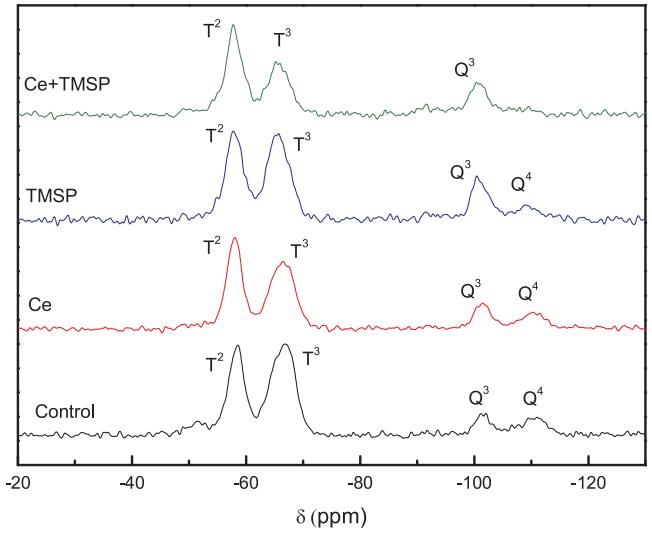

Fig. 4. Solid state ^{29}Si NMR spectra of gels from synthesis Control, Ce, TMSP, Ce + TMSP.

The main objective of this project is to prove the hypothesis about the positive synergic effect on a sol-gel coating doped with an inhibitor and a cross-linking agent. As inhibitor of the corrosion a cerium salt, namely a hexahydratated cerium nitrate, was employed; and as cross-linking agent a phosphorus compound, namely tris(trimethylsilyl) phosphite. Four sol-gel coatings were prepared: 1) the undoped coating; 2) the coating doped with the inhibitor; 3) the coating doped with the cross-linking agent; and 4) the coating doped with both, the inhibitor and the cross-linking agent.

2. Experimental

2.1. Materials and sample preparation

Titanium substrates were prepared by a conventional powder metallurgy route applying a cold uniaxial charge of 14.4 ton/cm^2 followed by a sintering step under high vacuum (10^{-5} mbar) at 1100 °C for 60 min as we have done in previous works [6,7]. The starting titanium powders with a particle size below 63 μm were supplied by GfEMetalleund Materialien GmbH. Prior to the application of the sol-gel coating, the metallic substrates were ground with SiC paper up to 180 grit and cleaned ultrasonically in alcohol and dried.

Sols were prepared starting from a mixture of 2 mol of (3-glycidyloxypropyl)trimethoxysilane (GPTMS, 98% from Sigma-Aldrich) and 1 mol of tetraethylorthosilane (TEOS, 98% from Sigma-Aldrich). This molar ratio has been selected based on a work [22] where Kim EK., et al. reported that higher contents of GPTMS than TEOS avoided cracks on the coatings. Ethanol and water were added in a molar ratio silane/ethanol/water of 1/3/3. Sols were stirred until the viscosity of the solution was such that it was adequate to coat the titanium by dip-coating. Four different sol-gel coatings were prepared as listed in Table 1. All the species were mixed before the addition of water. The latter is the reactive that starts the hydrolysis-condensation reaction. Cerium nitrate $Ce(NO_3)_3{\cdot}6H_2O$ and tris(trimethylsilyl)phosphite (TMSP) were used as received from Sigma-Aldrich.

Once the sol-gel synthesis was optimized by FTIR, substrates were coated on the metallic substrate, the protective layer was applied on the titanium samples by dipping them into the solutions at a speed of 100 mm min^{-1} for 15 s and retracting them with the same speed. Finally samples were dried at room temperature for 60 min, followed by thermal treatment at 60 °C for 17 h inside an oven.

2.2. Instruments

The evolution of the hydrolysis-condensation reaction was monitored by FTIR spectral analysis. Each sample was prepared by adding a sol-gel synthesis's drop to a pressed KBr disc. Spectra were recorded with a Perkin Elmer spectrum GX FT-IR System at room temperature covering the wave number range of 4000–500 cm^{-1} and with a resolution of 4 cm^{-1}.

The viscosity of sols was measured using a HAAKE ViscotesteriQ from Thermo Scientific with a parallel plate geometry and profiled surfaces. First, the viscosity was obtained by controlling the shear rate from 1 to 600 s^{-1}. And second, the viscosity was recorded for 30 s at fixed shear rates of 100, 200, 300, 400, 500 and 600 s^{-1}. Similar and stable values were obtained with the different share rates applied and a mean viscosity value from all the tests was calculated.

Gels were dried at room temperature for 7 days and ground in an agate mortar prior to the characterization by TGA and ^{29}Si-NMR. TGA were performed using the model Pyris™ 1 TGA from PerkinElmer. Around 20 mg of the dry gel was placed on alumina crucibles and heated at a 10 °C/min rate from 30 to 900 °C in air atmosphere. Measurements were made by duplicated. The ^{29}Si-NMR spectra were recorded in a Bruker AVANCE 400 spectrometer equipped with fast Fourier transform unit. Frequency used was 79.48 MHz (9.4T). Samples were spun at 10 kHz around an axis inclined 54°44′ with respect to the external magnetic field. Spectra were acquired with a pulse length of 5 μs (90 ° pulse), a relaxation delay of 10 s was used and 6000 accumulations were acquired. Spectra were referenced to TMS.

Thickness of films was measured using an ultrasonic thickness NEURTEK instrument. Electrochemical impedance spectroscopy (EIS)

Table 4
Relative proportions of T and Q species obtained from Fig. 4.

Synthesis	Relative proportion (%)				Ratio(%)	
	T^2	T^3	Q^3	Q^4	T^n	Q^n
Control	49.7	50.3	55.0	44.9	82.8	17.2
Ce	57.6	42.3	61.5	38.5	79.9	20.1
TMSP	50.7	49.3	75.6	24.3	75.4	24.6
Ce + TMSP	63.8	36.2	100	–	81.5	18.4

measurements were performed in the conventional three-electrode cell arrangement, using an Ag/AgCl/KCl (3 M) electrode as reference (E_0 = +0.210 V vs. NHE), and a platinum wire as counter electrode. A surface area of 0.38 cm^2 of the working electrode was exposed to the electrolyte. Impedance spectra were recorded using an AutolabPGSTAT302N potentiostat/galvanostat. The cell was placed in a Faraday cage to avoid external interferences from electromagnetic fields and wandering currents. Upon immersion in naturally aerated 5 mM NaCl solution at ambient temperature (20.5 °C ± 2 °C), the samples were left unpolarised for 24 h to attain a stable Open Circuit Potential (OCP) in the test solution. Impedance measurements were subsequently performed at regular intervals for 24 h using an amplitude of 10 mV with respect to OCP, and a frequency scan ranging from 10 kHz to 10 mHz, the values spaced logarithmically with 10 points per decade. OCP was recorded for 10 min before and after each impedance measurement in order to monitor the stability of the coatings. EIS data were fitted and analysed in terms of equivalent circuits (EC) using ZView software (Scribner Associates, Charlottesville, VA, USA) to obtain the relevant impedance parameters.

3. Results and discussion

3.1. Characterization of hybrid sols

FTIR is sensitive analytical method for identifying functional groups related with the hydrolysis and condensation reactions that occurs during the sol-gel process [23]. Fig. 1 shows FTIR spectra for the four syntheses analysed at different reactions times and Table 2 summarizes the most relevant bond-type signals associated with the hydrolysis and condensation reactions. During hydrolysis Si-OH bonds are (Table 3) created however, is not possible to distinguish its formation because a broad band related to the vibration modes of OH groups from water, silanols and ethanol overlap the Si-OH signal [24]. Strong bands between 1000 and 1200 cm^{-1} appeared in all spectra at different times depending on the synthesis. According to bibliography this facts evidence the creation of Si-O-Si bonds corresponding to condensation [23].

Synthesis doped with TMSP and Ce-TMSP has the fastest condensation rates. At 48 h it is possible to appreciate the condensation signals at 1185 cm^{-1}. On the other hand Control and Ce syntheses required 72 h to achieve this stage. The viscosity evolution of sols from the different synthesis is depicted in Fig. 2. Sols showed a gradual increment in viscosity until a critical point was reached at 72 h. At that point (72 h) the viscosity of TMSP sol increased one order of magnitude and it is associated with the condensation reaction of the gel process [25]. Ce-TMSP shows, however, a slightly shift similar to Control and sols containing cerium. TMSP acts as a cross-linking agent accelerating the condensation process, therefore the gelification time is shorter (less than 72 h) comparing to Control and Ce sols. Table 2 summarizes the mean viscosity values at different share rates (300, 400, 500, 600 and 700 s^{-1}).

3.2. Characterization of xerogels

Thermogravimetric analysis and their derivate of dry gels are shown in Fig. 3. Three different degradation stages for the four gels are revealed. The first stage was observed around 220 °C with similar mass losses (0.08–0.09%) for all gels. This degradation is associated to the separation of organic compounds of TEOS and GPTMS and volatile compounds such as CO_2 and H_2O [26–28]. The second degradation stage was observed at 407–409 °C with mass losses of 44.2 and 41.3% for Control and Ce respectively and 51.1% for TMSP and Ce-TMSP this signal is associate to the volatilization of unreacted oligomers and precursors of the silane (i.e., Si—OH uncondensed groups). Finally the third degradation step is at 519 °C which is ascribed to the degradation

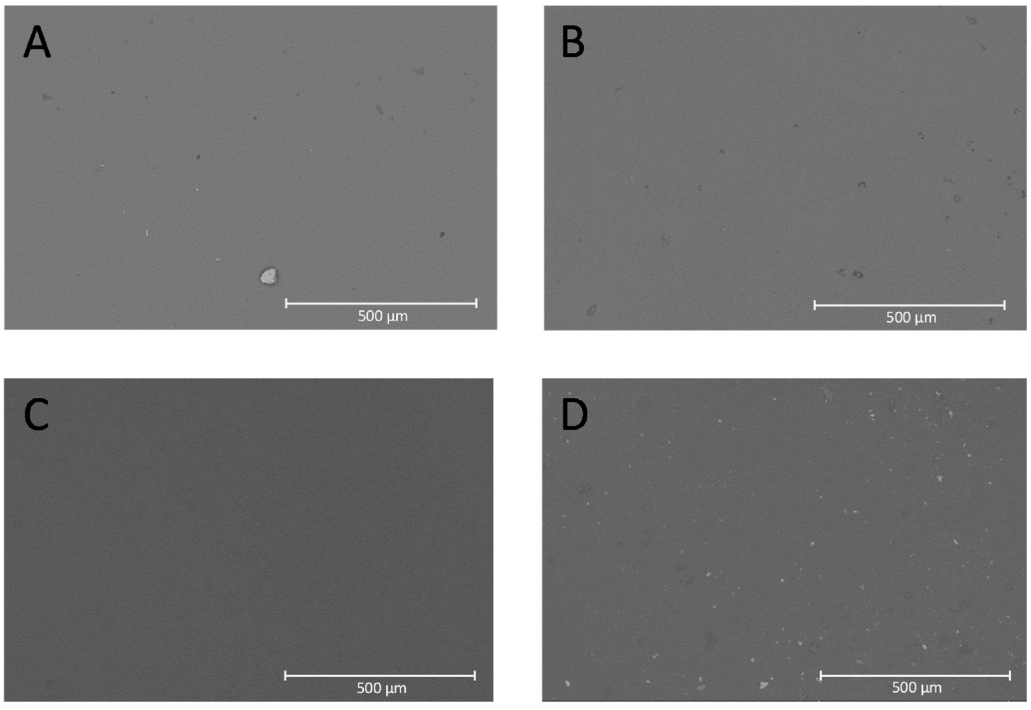

Fig. 5. Micrographs of coatings A) Control, B) Ce, C) TMSP, and D) Ce + TMSP.

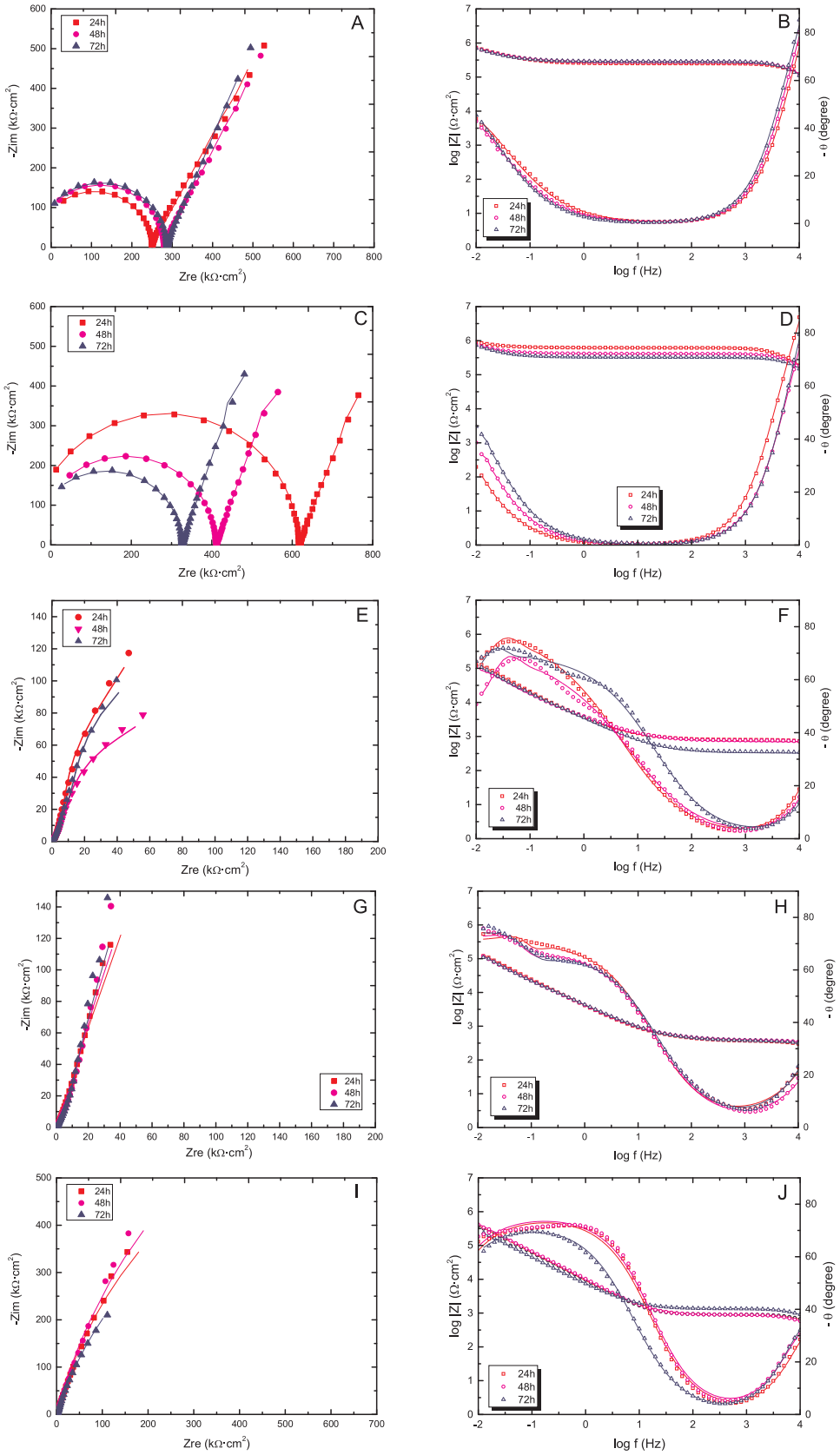

Fig. 6. Measured (discrete points) and fitted (solid lines) impedance spectrum of coatings: A-B) control C-D) Ce; E-F) TMSP; G-H) Ce + TMSP and I-J) Titanium after 24 h, 48 h and 72 h of exposure to 5 mM NaCl solution. Frequency range applied: 10^{4} Hz to 10^{-2} Hz.

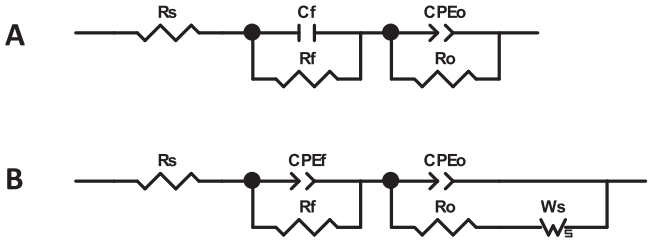

Fig. 7. Equivalent circuits for: A) Titanium and first set of coatings (Control and Ce), and B) second set of coatings (TMSP and Ce + TMSP).

of remaining organic groups from the starting precursors of the sol-gel network. The total mass left from synthesis control after achieving 850 °C was 51.2%. The addition of cerium to the sol-gel didn't affect the thermal stability of the network. However, the addition of TMSP and Ce + TMSP presented higher total mass loss.

The Si^{29}-NMR in the solid state has been used in order to characterize the inorganic structure of the four syntheses. This technique allows the determination of the environment of the silicon atoms and therefore it can provide details on the degree of hydrolysis and polycondensation [29]. According with the silane precursors used, two species can be identified: T^n peaks signals are attributed to GPTMS with three hydrolysable groups ($R\text{-}Si\text{-}(OH)_3$), and Q^n signals from TEOS with four hydrolysable groups ($Si\text{-}(OH)_4$), where n can have values of 0, 1, 2, 3 or 4 depending on the amount of siloxane bonds created from the hydrolysable groups [30]. T^n signals, derived from organoalkoxysilanes, appear in the range −40 to −80 ppm and Q^n signals from TEOS appear between −80 and −120 ppm. Hydrolysis and further condensation is achieved when signals T^3 and Q^4 appear in the ^{29}Si NMR spectrum [29]. Non-hydrolysable species (i.e., T^0 or Q^0) were identified meaning a good cross-linkage of sols was obtained. Fig. 4 shows the spectra for each synthesis and Table 4 summarizes the contribution of T and Q species to the siloxane bond of each synthesis. Regarding the control, GPTMS presented a higher contribution to the siloxane network than TEOS; 82.8% against 17.2%. It seems that even though the molar quantity of GPTMS is double the one of TEOS, the organic chain of GPTMS allowed a better hydrolization of the species. The addition of Cerium, TMSP and Ce + TMSP did not compromised the nature of the sol-gel cross-linkage. It is worth to remark that the addition of both, Ce + TMSP decreased Q^4 contributions. This might be due to the creations of new bonds (P—O—Si) between the silane precursors and the P compound as a result of a reaction of the different reactive.

3.3. Characterization of the hybrid sol-gel coatings

Fig. 5 shows the surface and the composition of the coatings prepared before EIS tests. All the coatings reveal a surface without cracks and completely covered by the coating. However some dark spots were observed on the surface of Control, Ce, TMSP and Ce + TMSP. These are agglomerations of particles during the drying step of the sol-gel process meaning that further optimization of the drying step is required to obtain a more homogenous surface. However, for a preliminary electrochemical study having a full surface covered with the coating is enough.

3.4. Evaluation of the corrosion resistance of coatings

The synergetic electrochemical effect of TMSP and cerium has been evaluated by electrochemical impedance spectroscopy. Tests were recorded at their corresponding open circuit potential (OCP) after 24 h immersed in 5 mM NaCl solution. Before and after each impedance test, OCP was recorded and differences between the starting and final OCP remained smaller than 50 mV in all cases. Fig. 6 depicts EIS data for all the coatings prepared where Nyquist (complex vs real impedance) and Bode (impedance modulus and phase angle vs frequency) plots are shown. Coatings are classified into first or second set of coating depending on the electrochemical data recorded and 2 different equivalent circuits were proposed to fit each set of coatings. Thus, equivalent circuit of Fig. 7A was used to fit data of the 1st set of coatings, while equivalent circuit of Fig. 7B was used to fit the second set of coatings. Both set of coatings showed two time constants but the second set of coatings also presented a diffusion process, which was taken into account by adding a finite element Warburg (W). The good agreement between fitted and measured data is shown in table with a chi-square smaller than 10^{-3}. At first glance it can be observed 2 different electrochemical behaviors.

Control and Ce coating (1st set of coatings) had the same features (Fig. 6A–D) showing two time constants. The time constant identified at high frequencies is represented by the ideal capacitor of the silane coating (C_f) and its resistance (R_f). The second time constant is represented by a constant phase element (CPE_o) and a resistance (R_o) which is associated to the interface electrolyte/metal response due to the presence of pores or degradation of the coating. It is worth to remark the stability of these coatings within the exposed time to the electrolyte: control remained almost unaltered whereas Ce showed a slightly decrease on the barrier properties of the coating. The decrease on the barrier properties of Ce was evidenced by the decrease on both the impedance modulus (Bode plot) and the amplitude of the arc (Nyquist plot). Even though Ce reduced its barrier properties with time, the impedance obtained was always above the one recorded by the control.

TMSP and Ce + TMSP data, the 2nd set of coatings, was satisfactorily fitted using the equivalent circuits shown in Fig. 7B, which describes the barrier characteristics of an unsealed non-homogenous film [31]. The equivalent circuit of these systems correspond to the interaction metal/electrolyte due to presence of pores in the film, and

Table 5
Parameters of the equivalent circuit for silane coated titanium immersed in 5 mM NaCl for 72 h.

Samples	1st set of coating						2nd set of coating					
	Control			Ce			TMSP			Ce + TMSP		
Time (h)	24	48	72	24	48	72	24	48	72	24	48	72
Log $\|Z\|_{LF}$	5.86	5.85	5.85	5.96	5.88	5.86	5.17	5.04	5.11	5.18	5.15	5.17
$R_f \times 10^3/\Omega cm^2$	2800	3100	3200	6600	4500	3700	1.6	0.54	0.52	1.1	0.90	0.30
$C_f/CPE_f\text{-}T_1 \times 10^{-9}/Fcm^{-2}$	0.100	0.103	0.111	0.072	0.072	0.081	14	7.26	12	131	33	505
$CPE_f\text{-}P_1$							0.80	1	0.92	0.63	0.77	0.62
$R_o \times 10^3/\Omega cm^2$	5500	9200	13000	11000	6600	8080	7.4	8.7	18	1.8	1.3	4.4
$CPE_o\text{-}T_2 \times 10^{-5}/Fcm^{-2}$	1,1	1,3	1,5	1.8	1.8	1.7	5.5	6	6.2	4.2	4.3	4.7
$CPE_o\text{-}P_2$	0.71	0.71	0.76	0.78	0.80	0.81	0.80	0.74	0.78	0.81	0.78	0.79
$W_s\text{-}R \times 10^5/cm^2$	–	–	–	–	–	–	5.7	2.9	6.9	14.1	6.4	6.7
$W_s\text{-}T/Fcm^{-2}$	–	–	–	–	–	–	13.4	9.5	15.3	57.7	31.8	27.8
$W_s\text{-}P_{f3}$	–	–	–	–	–	–	0.82	0.77	0.79	0.78	0.73	0.80
Chi-Sqr $\times 10^{-3}$	0.91	0.86	1.6	0.66	0.26	0.93	4.4	1.9	1.1	0.85	1.6	4.1

an unsealed outer layer due to the silane contribution [32], [33]. It is also remarkable that with the immersion time, the second set of coatings revealed the third time constant more clearly indicating that the electrolyte reached the titanium oxide. This phenomenon was taken into account by adding the Warburg element. The corrosion resistance of the 2nd set of coatings, which is represented by the impedance modulus, is almost one order of magnitude below the impedance recorded by the 1st set of coatings.

In order to understand better the electrochemical behaviour of the coatings, the uncoated Ti was also studied. Fig. 6I–J shows plots for Ti and data was fitted using equivalent circuit of Fig. 7A.

Table 5 summarizes the parameters evaluated from the equivalent circuit. It was observed that the second set of coatings have lower barrier resistance properties than the uncoated titanium (Log $|Z|_{LF}$ titanium: 5.56; 5.61; 5.33 for 24 h, 48 h and 72 h respectively). This decrease on the electrochemical behaviour may be caused by the presence of pores on the coating that increases the heterogeneous electrochemical response induced by the TMSP component. The first set of coatings however, showed an improvement on the impedance values.

Concerning the 1st set of coatings, which showed a more solid and homogenous surface, an ideal capacitor C_f was satisfactory introduced in the first time constant rather than a constant phase element. These coatings presented insulating features as it can be confirmed with the low value obtained in C_f, with an order of magnitude of 10^{-11}. The 2nd set of coating presented a higher value (with values between 10^{-7} and 10^{-9}) with lower insulating features due to the presence of porous in the coating surface. C_f and CPE_f-T_1 slightly increased with the immersion time indicating an uptake of water, which is related to the first stage of a coating degradation. Comparing the resistance of the coating (R_f), the 1st set of coating showed a value 2–3 orders of magnitude higher than the second set of coatings. Again, this supports the fact that Control and Ce coatings were denser and more insulating than TMSP and Ce + TMSP coatings.

Regarding the second time constant there are remarkable differences between the 1st and 2nd set of coatings on the resistance (R_o). R_o, which represents the resistance between the interface metal/electrolyte, is 3-2 orders of magnitude up in the case of the 1st set of coatings, meaning that titanium is completely covered by the sol-gel coating. The lower R_o values obtained in the 2nd set of coatings, revealed that the coating was started its degradation and that part of the substrate is already in contact with the electrolyte. This statement is supported by the addition of the Warburg element on the second set of coatings.

4. Conclusions

Due to hybrid sol-gel characterization by FTIR and viscosity we could concluded that small quantities of TMSP accelerate the condensation reaction due to it is possible to appreciate the Si-O-Si bands at 48 h and the increment on the viscosity through time.

Thermal characterization of xerogels showed that addition of Ce-TMSP, TMSP and Ce decrease the thermal stability behaviour of the sol-gel network. ^{29}Si-NMR results showed that addition of TMSP and Ce decrease Q^4 signals contributions until Ce-TMSP where non Q^4 signals has been found. It might be due to the creations of new bonds (P—O—Si) between the silane precursors and the P compound as a result of a reaction of the different reactive. The electrochemical characterization showed that the Control coating presented stable barrier properties within 72 h immersed in 5 mM NaCl. Two times constants were identified and data was fitted using an equivalent circuit that corresponds to dense, insulating and homogenous coatings. The addition of Cerium Nitrate as inhibitor to the sol-gel (Ce coating) followed the same electrochemical features than the Control coating however it remains less stable with time. The addition of tris(trimethylsilyl)phosphite (TMSP coating), however, showed remarkable differences if compared with the Control. Three times constants were identified and the equivalent circuit proposed to fit the data corresponds to unsealed coatings. The phosphorus compound decreased considerably the good electrochemical properties obtained with the undoped coating. Finally, the synergy between the Cerium inhibitor and the TMSP cross-linking agent (Ce-TMSP coating) was not positive because the electrochemical behaviour was dominated by the phosphorus compound over the Cerium.

Acknowledgements

The authors acknowledge the financial support from the Regional Government of Madrid through the program MULTIMAT-CHALLENGE (S2013/MIT-2862).

The authors acknowledge the financial support from the European Union and Government of Spain through the program RETOS-COLABORACIÓN. RECORD (RTC-2015-3513-S)

References

[1] M.L.T. Cossio, et al., Titanium, Manuf. Technol. Aerosp. Struct. Mater. XXXIII (2) (2012) 81–87.

[2] A.A. El Hadad, et al., Biocompatibility and corrosion protection behaviour of hydroxyapatite sol-gel-derived coatings on Ti6Al4 V alloy, Materials (Basel) 10 (2) (2017).

[3] M.J. Juan-Díaz, et al., Study of the degradation of hybrid sol-gel coatings in aqueous medium, Prog. Org. Coat. 77 (11) (2014) 1799–1806.

[4] A. Amherd Hidalgo, R. Frykholm, T. Ebel, F. Pyczak, Powder metallurgy strategies to improve properties and processing of titanium alloys: a review, Adv. Eng. Mater. 19 (6) (2017) 1–14.

[5] R.G. Neves, B. Ferrari, A.J. Sanchez-Herencia, E. Gordo, Colloidal approach for the design of Ti powders sinterable at low temperature, Mater. Lett. 107 (2013) 75–78.

[6] S.A. Tsipas, E. Gordo, A. Jimenez-Morales, Oxidation and corrosion protection by halide treatment of powder metallurgy Ti and Ti6Al4 V alloy, Corros. Sci. 88 (2014) 263–274.

[7] J. Ureña, et al., Surface modification of powder metallurgy titanium by colloidal techniques and diffusion processes for biomedical applications, Adv. Eng. Mater. 19 (6) (2017) 1–8.

[8] D.J. Carbonell, A. García-Casas, J. Izquierdo, R.M. Souto, J.C. Galván, A. Jiménez-Morales, Scanning electrochemical microscopy characterization of sol-gel coatings applied on AA2024-T3 substrate for corrosion protection, Corros. Sci. 111 (2016) 625–636.

[9] D. Balgude, A. Sabnis, Sol-gel derived hybrid coatings as an environment friendly surface treatment for corrosion protection of metals and their alloys, J. Sol-Gel Sci. Technol. 64 (1) (2012) 124–134.

[10] R.B. Vignesh, J. Balaji, M.G. Sethuraman, Surface modification, characterization and corrosion protection of 1,3-diphenylthiourea doped sol-gel coating on alumi-nium, Prog. Org. Coat. 111 (May) (2017) 112–123.

[11] R.Z. Zand, K. Verbeken, A. Adriaens, Influence of the cerium concentration on the corrosion performance of ce-doped silica hybrid coatings on hot dip galvanized steel substrates, Int. J. Electrochem. Sci. 8 (1) (2013) 548–563.

[12] R.-G. Hu, S. Zhang, J.-F. Bu, C.-J. Lin, G.-L. Song, Progress in Organic Coatings Recent progress in corrosion protection of magnesium alloys by organic coatings, Prog. Org. Coat. 3 (2012) 129–141.

[13] C. Motte, M. Poelman, A. Roobroeck, M. Fedel, F. Deflorian, M.G. Olivier, Improvement of corrosion protection offered to galvanized steel by incorporation of lanthanide modified nanoclays in silane layer, Prog. Org. Coat. 74 (2) (2012) 326–333.

[14] M. Hernandez-Escolano, X. Ramis, A. Jimenez-Morales, M. Juan-D??az, J. Suay, Study of the thermal degradation of bioactive sol-gel coatings for the optimization of its curing process, J. Therm. Anal. Calorim. 107 (2) (2012) 499–508.

[15] C.-W. Lee, H.-S. Park, J.-G. Kim, M.-S. Gong, Humidity sensitivity of hybrid polyelectrolytes prepared by the sol-gel process, Macromol. Res. 13 (2) (2005) 96–101.

[16] S. Zheng, J. Li, Inorganic-organic sol gel hybrid coatings for corrosion protection of metals, J. Sol-Gel Sci. Technol. 54 (2) (2010) 174–187.

[17] S.V. Lamaka, et al., Novel hybrid sol-gel coatings for corrosion protection of AZ31 B magnesium alloy, Electrochim. Acta 53 (14) (2008) 4773–4783.

[18] A.N. Khramov, V.N. Balbyshev, L.S. Kasten, R.A. Mantz, Sol-gel coatings with phosphonate functionalities for surface modification of magnesium alloys, Thin Solid Films 2 (2006) 174–181.

[19] T.G. Harvey, et al., The effect of inhibitor structure on the corrosion of AA2024 and AA7075, Corros. Sci. 53 (6) (2011) 2184–2190.

[21] A. De Nicolò, et al., Cerium conversion coating and sol-gel multilayer system for corrosion protection of AA6060, Surf. Coat. Technol. 287 (3) (2016) 33–43.

[22] E.K. Kim, J. Won, J. young Do, S.D. Kim, Y.S. Kang, Effects of silica nanoparticle and GPTMS addition on TEOS-based stone consolidants, J. Cult. Herit. 10 (2) (2009) 214–221.

[23] A.A. El Hadad, D. Carbonell, V. Barranco, A. Jiménez-Morales, B. Casal, J.C. Galván, Preparation of sol-gel hybrid materials from γ-methacryloxypropyltrimethoxysilane and tetramethyl orthosilicate: study of the hydrolysis and condensation reactions, Colloid Polym. Sci. 289 (17–18) (2011) 1875–1883.

[24] F. Romero-Gavilán, et al., Control of the degradation of silica sol-gel hybrid coatings for metal implants prepared by the triple combination of alkoxysilanes, J. Non.

Cryst. Solids 453 (2016) 66–73.
[25] L.M. Rueda, C. Nieves, C.A. Hernández Barrios, A.E. Coy, F. Viejo, Design of TEOS-GPTMS sol-gel coatings on rare-earth magnesium alloys employed in the manufacture of orthopaedic implants, J. Phys. Conf. Ser. 687 (2016) 12013.
[26] H. Li, S. Liu, J. Zhao, D. Li, Y. Yuan, Thermal degradation behaviors of polydimethylsiloxane-graft-poly(methyl methacrylate), Thermochim. Acta 573 (2013) 32–38.
[27] G. Camino, S.M. Lomakin, M. Lageard, Thermal polydimethylsiloxane degradation. part 2. the degradation mechanisms, Polymer (Guildf) 43 (7) (2002) 2011–2015.
[28] M. Criado, I. Sobrados, J. Sanz, Polymerization of hybrid organic-inorganic materials from several silicon compounds followed by TGA/DTA, FTIR and NMR techniques, Prog. Org. Coat. 77 (4) (2014) 880–891.
[29] X. Fernández-Francos, A. Serra, X. Ramis, Epoxy sol-gel hybrid thermosets, Coatings 6 (8) (2016) 1–19.
[30] R.J. Hook, A 29Si NMR study of the sol-gel polymerisation rates of substituted ethoxysilanes, J. Non. Cryst. Solids 2 (1996) 1–15.
[31] F. Mansfeld, Analysis and interpretation of EIS data for metals and alloys–an introduction to electrochemical impedance measurement, Solartron Anal. 155 (26) (1999) 1–77.
[32] M.G. Olivier, et al., Study of the effect of nanoclay incorporation on the rheological properties and corrosion protection by a silane layer, Prog. Org. Coat. 2 (2011) 15–20.
[33] V. Dalmoro, J.H.Z. dos Santos, C. Alemán, D.S. Azambuja, An assessment of the corrosion protection of AA2024-T3 treated with vinyltrimethoxysilane/(3-glycidyloxypropyl)trimethoxysilane, Corros. Sci. 92 (2015) 200–208.